Journal of Applied Electrochemistry **34**: 383–389, 2004.

Electrochemical properties of cathode materials $LiNi_{1-y}Co_yO_2$ synthesized using various starting materials

M.Y. SONG*, H. RIM and E. BANG
Division of Advanced Materials Engineering, Research Center of Industrial Technology, Engineering Research Institute, Chonbuk National University, Jeonju 561-756, Republic of Korea
*(*author for correspondence, fax: +82 63 270 2386, e-mail: songmy@moak.chonbuk.ac.kr)*

Received 9 September 2002; accepted in revised form 21 October 2003

Key words: cycling performance, discharge capacity, lattice destruction, $LiNi_{1-y}Co_yO_2$, solid-state reaction

Abstract

$LiNi_{1-y}Co_yO_2$ samples were synthesized at 800 °C and 850 °C, by the solid-state reaction method, using the starting materials $LiOH \cdot H_2O$, Li_2CO_3, NiO, $NiCO_3$, Co_3O_4 and $CoCO_3$. The $LiNi_{1-y}Co_yO_2$ synthesized using Li_2CO_3, NiO and Co_3O_4 exhibited the α-$NaFeO_2$ structure of the rhombohedral system (space group $R\bar{3}m$). As the Co content increased, the lattice parameters *a* and *c* decreased. The reason is that the radius of the Co ion is smaller than that of the Ni ion. The increase in c/a shows that a two-dimensional structure develops better as the Co content increases. The $LiNi_{0.7}Co_{0.3}O_2$ synthesized at 800 °C using $LiOH \cdot H_2O$, NiO and Co_3O_4 exhibited a larger first discharge capacity of 162 mAh g^{-1} than the other samples. The cycling performances of the samples with the first discharge capacity larger than 150 mAh g^{-1} were investigated. $LiNi_{0.9}Co_{0.1}O_2$ synthesized at 850 °C using Li_2CO_3, NiO and Co_3O_4 showed excellent cycling performance. Samples with larger first discharge capacity will have a greater tendency for lattice destruction due to expansion and contraction during intercalation and deintercalation, than samples with smaller first discharge capacity. As the first discharge capacity increases, the capacity fading rate thus increases.

1. Introduction

Transition metal oxides such as $LiCoO_2$ [1–4], $LiNiO_2$ [5–9] and $LiMn_2O_4$ [10–17] have been investigated in order to apply them as positive electrode (cathode) materials for lithium secondary batteries. $LiMn_2O_4$ is very cheap and does not cause environmental pollution, but its cycle performance is not good. Layered $LiNiO_2$ and $LiCoO_2$ exhibit complementary behaviour; $LiCoO_2$ is easy to synthesize by the solid-state method, but is very expensive when compared with $LiNiO_2$. However, $LiNiO_2$ is quite difficult to synthesize as a result of a tendency to nonstoichiometry due to the presence of an excess of nickel.

A convenient way to overcome these drawbacks may be to use mixed phases with $LiNi_{1-y}Co_yO_2$ composition because the presence of cobalt stabilizes the structure in a strictly two-dimensional fashion, thus giving good reversibility of the intercalation and deintercalation reactions [18–27].

In this work $LiNi_{1-y}Co_yO_2$ ($y = 0.1$, 0.3, 0.5, 0.7 and 1.0) were synthesized by the solid-state reaction method at different temperatures using various starting materials. The crystal structure, the electrochemical properties and the microstructure of the synthesized samples were examined. The synthesis conditions (starting materials, compositions and temperatures) producing good electrochemical properties were investigated.

2. Experimental details

$LiOH \cdot H_2O$, Li_2CO_3, NiO, $NiCO_3$, Co_3O_4 and $CoCO_3$ were used as starting materials in order to synthesize $LiNi_{1-y}Co_yO_2$ by the solid-state reaction method. All the starting materials (assay 99.9%) were purchased from Aldrich Co.

The experimental procedure is shown schematically in Figure 1. The mixture of starting materials with composition $Li_{1.1}Ni_{1-y}Co_yO_2$ ($y = 0.1$, 0.3, 0.5, 0.7 and 1.0) was well mixed and pelletized. Excess Li was added to compensate for the evaporated Li during preparation. This pellet was heat-treated in air at 650 °C for 20 h. It was then well ground, mixed, pelletized and calcined at 800 °C or 850 °C for 20 h. This pellet was cooled at a rate of 50 °C min^{-1}, ground, mixed and again pelletized. It was calcined again at 800 °C or 850 °C for 20 h.

The phase identification of the synthesized samples was carried out by X-ray diffraction (XRD) analysis using CuK_α radiation (Mac-Science Co.). The scanning rate was 16° min^{-1} and the scanning range of diffraction angle (2θ) was $10° \leqslant 2\theta \leqslant 70°$ The morphologies of

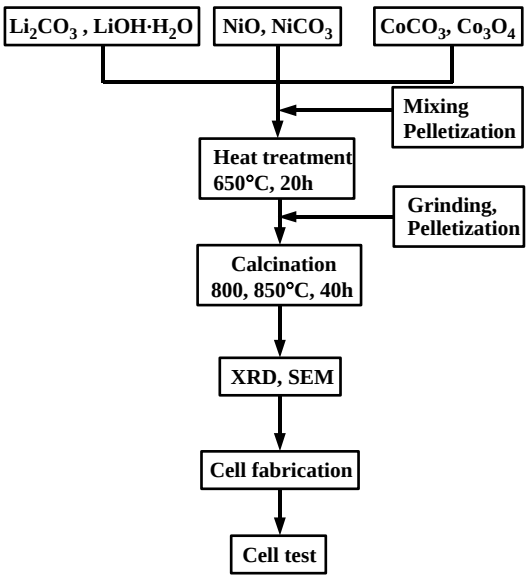

Fig. 1. Experimental procedure.

the samples were observed using a scanning electron microscope (SEM).

The electrochemical cells consisted of $LiNi_{1-y}Co_yO_2$ as a positive electrode, Li foil as a negative electrode, and an electrolyte of 1 M $LiPF_6$ in a 1:1 (volume ratio) mixture of ethylene carbonate (EC) and dimethyl carbonate (DMC). Whatman glass-fibre was used as the separator. The cells were assembled in an argon-filled dry box. To fabricate the positive electrode, 89 wt % synthesized oxide, 10 wt % acetylene black, and 1 wt % polytetrafluoroethylene (PTFE) binder were mixed in an agate mortar. All the electrochemical tests were performed at room temperature with a potentiostatic/galvanostatic system (Mac-Pile system, Bio-Logic Co.). The cells were cycled at a current density of 200 μA cm^{-2} between 3.2 and 4.3 V.

3. Results and discussion

Figure 2 shows the X-ray (CuK_α) diffraction patterns of the $LiNi_{1-y}Co_yO_2$ synthesized at 800 °C using Li_2CO_3, NiO and Co_3O_4. They were identified as the α-$NaFeO_2$ structure of the rhombohedral system (space group $R\bar{3}m$). As the Co content increases, the relative intensity of (003) increases. The reason is that the directionality to the *c*-axis improves since the $LiCoO_2$ layer increases in which Li and Co ions are in a completely-ordered arrangement, and the three-dimensional characteristics decrease which results from the substitution of Ni ions for Li sites like $LiNiO_2$.

Figure 3 shows the parameters of the hexagonal unit cell, *a* and *c*, with the degree of trigonal distortion, *c*/*a*, against Co content *y* in the $Li_xNi_{1-y}Co_yO_2$ synthesized at 800 °C using Li_2CO_3, NiO and Co_3O_4. As the Co content increases, the lattice parameters *a* and *c* decrease. The reason is that the radius of the Co ion (0.53 Å, low spin) is smaller than that of the Ni ion (0.60 Å, low spin). However, the *c*-axis is elongated when compared with the *a*-axis, showing that two-dimensional structures develop better than $LiNiO_2$.

Figure 4 shows the variations of the first discharge capacities of the synthesized samples with composition, starting materials and synthesis temperature. The $LiNi_{0.7}Co_{0.3}O_2$ synthesized at 800 °C using $LiOH \cdot H_2O$, NiO and Co_3O_4 exhibited the largest first discharge capacity 162 mAh g^{-1}. The $LiNi_{0.7}Co_{0.3}O_2$ synthesized

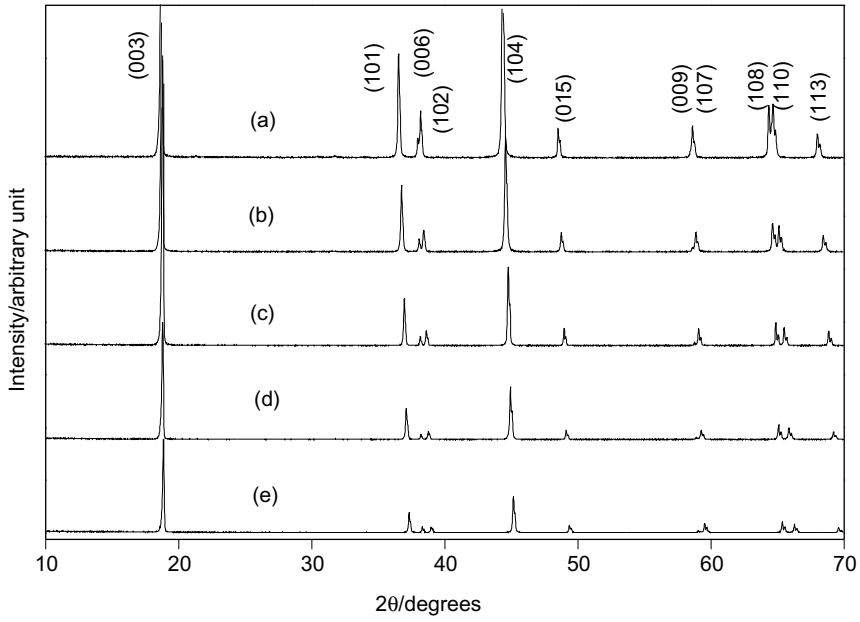

Fig. 2. X-ray (CuK_α) diffraction patterns of: (a) $LiNi_{0.9}Co_{0.1}O_2$, (b) $LiNi_{0.7}Co_{0.3}O_2$, (c) $LiNi_{0.5}Co_{0.5}O_2$, (d) $LiNi_{0.3}Co_{0.7}O_2$ and (e) $LiCoO_2$ synthesized at 800 °C using Li_2CO_3, NiO and Co_3O_4.

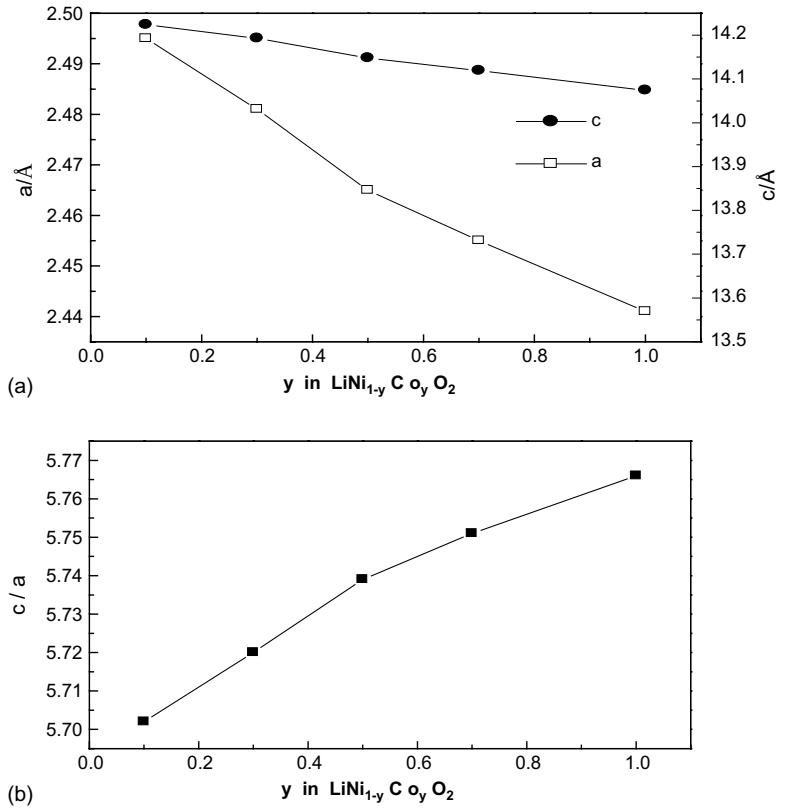

Fig. 3. Parameters of the hexagonal unit cell, *a*, *c* and degree of trigonal distortion, c/a, against Co content *y* in $Li_xNi_{1-y}Co_yO_2$: (a) hexagonal lattice parameters, *a*(□) and *c*(●), and (b) (*c*/*a*) ratio against Co content *y* in $LiNi_{1-y}Co_yO_2$ synthesized at 800 °C using Li_2Co_3, NiO and Co_3O_4.

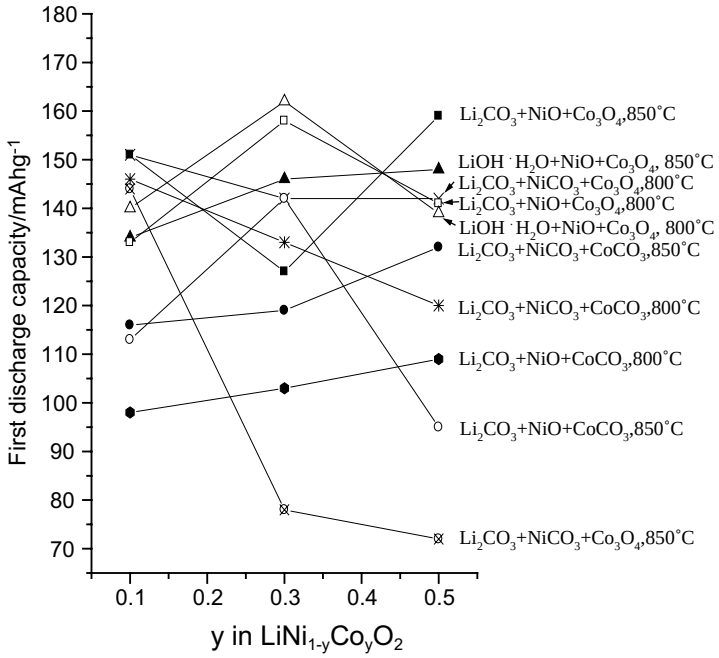

Fig. 4. Variations of the first discharge capacities of the synthesized samples with composition, starting materials and synthesis temperature.

at 800 °C using Li_2CO_3, NiO and Co_3O_4, the $LiNi_{0.5}Co_{0.5}O_2$ and the $LiNi_{0.9}Co_{0.1}O_2$ synthesized at 850 °C using Li_2CO_3, NiO and Co_3O_4, and the $LiNi_{0.9}Co_{0.1}O_2$ synthesized at 800 °C using Li_2CO_3, $NiCO_3$ and Co_3O_4, also exhibited first discharge capacities larger than 150 mAh g^{-1}.

Figure 5 shows the curves for voltage against *x* in $LiNi_{1-y}Co_yO_2$ of $Li/LiNi_{1-y}Co_yO_2$ cells synthesized at

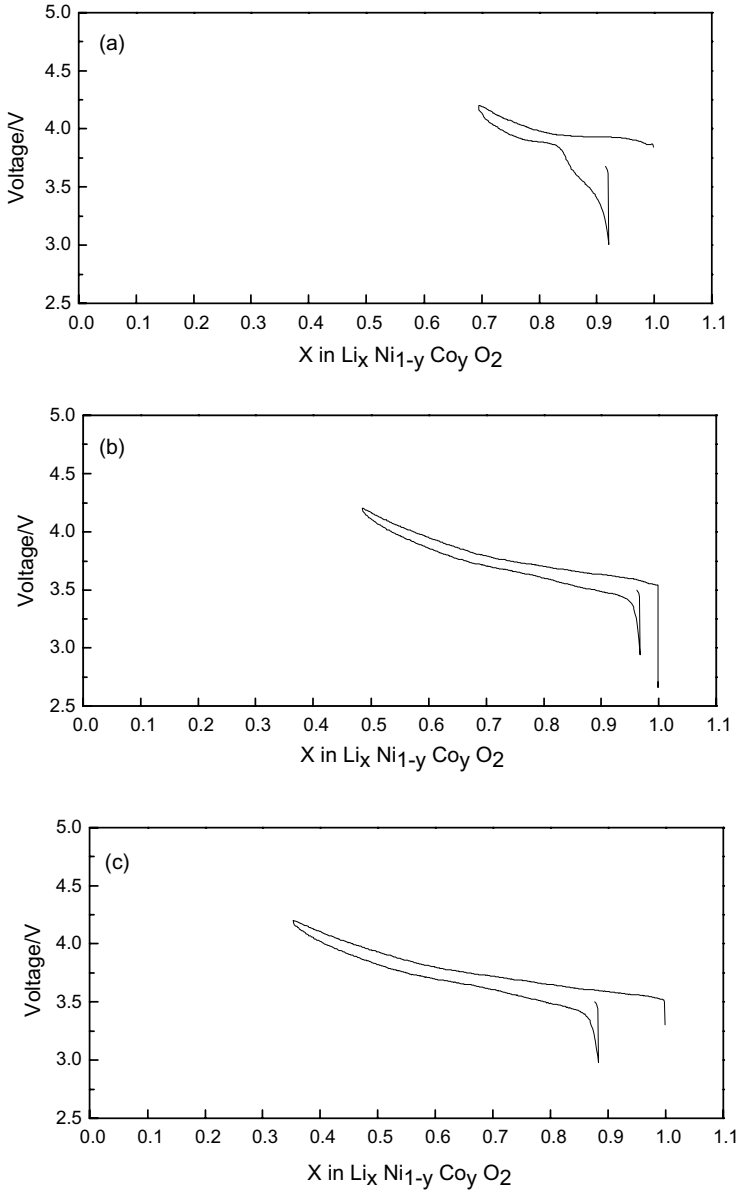

Fig. 5. Curves for voltage against x in $Li_xNi_{1-y}Co_yO_2$ synthesized at 850 °C using Li_2CO_3, $NiCO_3$ and $CoCO_3$ for the first cycle: (a) $y = 0.1$, (b) $y = 0.3$ and (c) $y = 0.5$.

850 °C using Li_2CO_3, $NiCO_3$ and $CoCO_3$ for the first cycle: (a) $y = 0.1$, (b) $y = 0.3$ and (c) $y = 0.5$. These samples exhibited relatively small first discharge capacities. The plateau in the voltage against x curve is not distinct.

Figure 6 shows the curves for voltage against x in $Li_xNi_{1-y}Co_yO_2$ of $Li/LiNi_{1-y}Co_yO_2$ cells using $LiNi_{1-y}Co_yO_2$ synthesized at 800 °C from Li_2CO_3, NiO and Co_3O_4 for (a) $y = 0.1$, (b) $y = 0.3$ and (c) $y = 0.5$. These samples exhibited relatively large first discharge capacities. The plateau in the voltage against x curve is more distinct as compared with the curves in Figure 5.

As compared with the quantity of deintercalated Li ions during the first charging, that of the intercalated Li ions during the first discharging is much smaller. It is considered that this is because, during the first charging, Li ions not only deintercalate from 3b sites but also come from Li atoms which may be contained in excess outside the 3b sites within the sample. During the first charging, deintercalation of Li ions from unstable 3b sites may destroy the $LiNiO_2$ structure (α-$NaFeO_2$ structure) and the quantity of Li ions from the Li atoms outside the 3b sites for the following charging will become much smaller as the number of cycles increases, leading to a smaller quantity of Li ions for the following intercalation.

Figure 7 shows the SEM micrographs of $LiNi_{1-y}Co_yO_2$ synthesized at 850 °C using Li_2CO_3, $NiCO_3$ and $CoCO_3$ for (a) $y = 0.1$, (b) $y = 0.3$ and (c) $y = 0.5$. These samples are the same as used for Figure 5. As the Co content increases the particle size becomes smaller. The particles for $y = 0.3$ have a slightly larger particle size than those for $y = 0.5$.

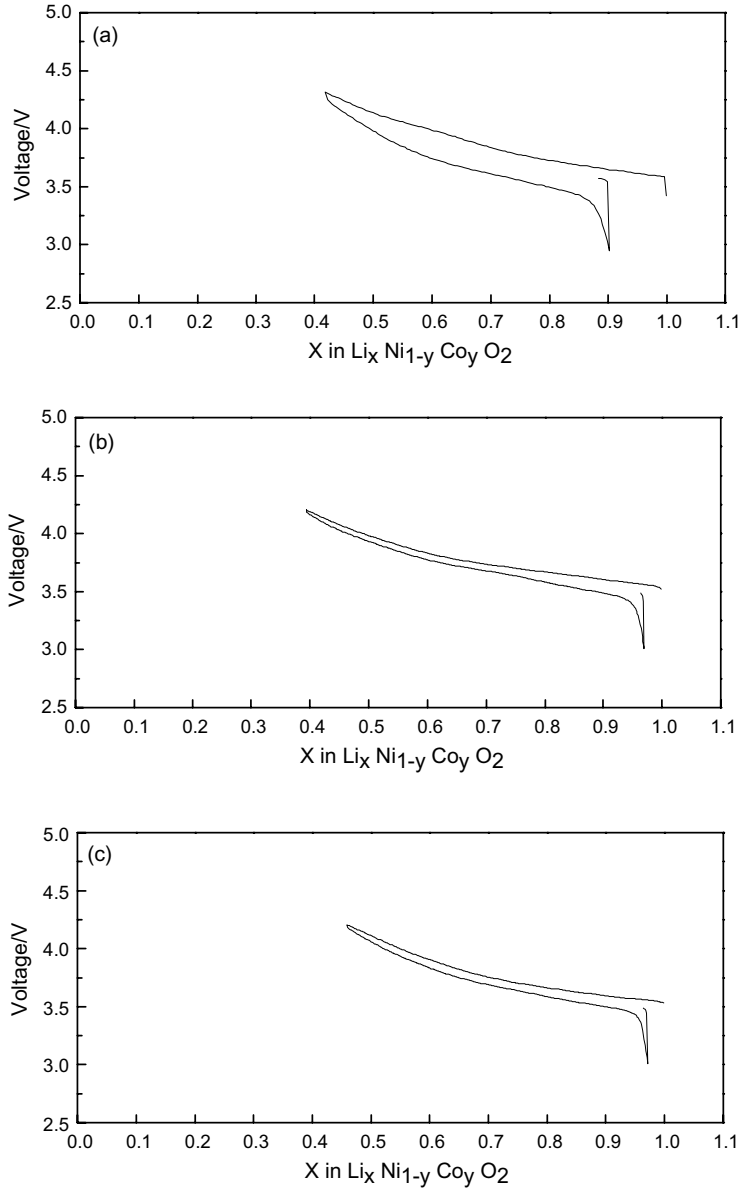

Fig. 6. Curves for voltage against x in $Li_xNi_{1-y}Co_yO_2$ synthesized at 800 °C using Li_2CO_3, NiO and Co_3O_4 for the first cycle: (a) $y = 0.1$, (b) $y = 0.3$ and (c) $y = 0.5$.

Figure 8 shows SEM micrographs of $LiNi_{1-y}Co_yO_2$ synthesized at 800 °C using Li_2CO_3, NiO and Co_3O_4 for (a) $y = 0.1$, (b) $y = 0.3$ and (c) $y = 0.5$. These samples are the same as used for Figure 6. When the value of y increases from $y = 0.1$ to 0.3, the particle size becomes somewhat smaller. The particles then grow a little larger when y increases from $y = 0.3$ to 0.5. The particles for each value of y have relatively uniform size.

Figure 9 shows the variations of the discharge capacities with the number of discharge cycles for samples having first discharge capacity larger than 150 mAh g^{-1}. $LiNi_{0.9}Co_{0.1}O_2$ synthesized at 850 °C using Li_2CO_3, NiO and Co_3O_4 exhibited excellent cycling performance with a discharge capacity of about 156 mAh g^{-1} at the 6th discharge cycle. $LiNi_{0.9}Co_{0.1}O_2$ synthesized at 800 °C using Li_2CO_3, $NiCO_3$ and Co_3O_4 also exhibited excellent cycling performance.

Figure 10 shows the variations of capacity fading rate with the first discharge capacity for samples having first discharge capacity larger than 150 mAh g^{-1}. The starting materials and the synthesis temperature are also indicated. As the first discharge capacity increases, the capacity fading rate increases. The expansion and contraction of the $LiNi_{1-y}Co_yO_2$ due to the intercalation and deintercalation make the unit cell strained and distorted. With cycling, the interstitial sites, and thus the $LiNi_{1-y}Co_yO_2$ structure, will be destroyed. This leads to capacity fading of $LiNi_{1-y}Co_yO_2$ with cycling. The sample with the larger first discharge capacity will experience the more severe lattice destruction than the sample with the smaller first discharge capacity, causing

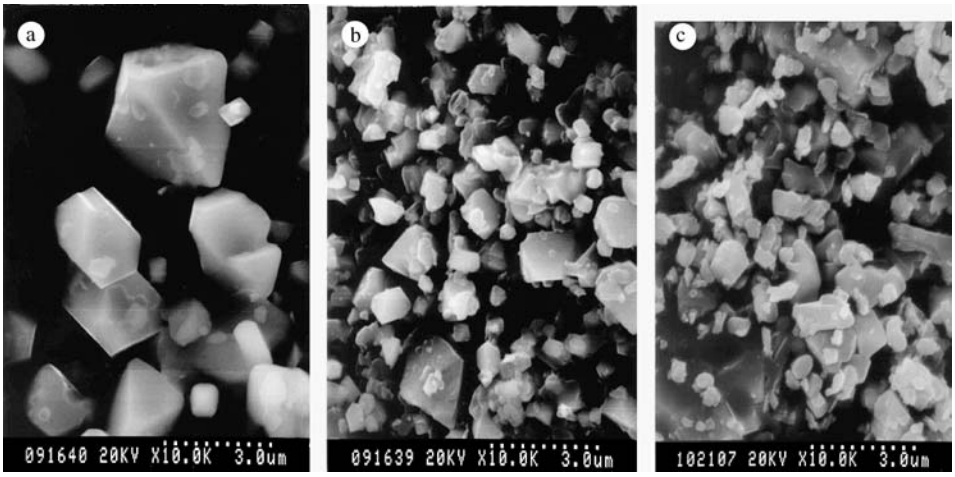

Fig. 7. SEM micrographs of $LiNi_{1-y}Co_yO_2$ synthesized at 850 °C using Li_2CO_3, $NiCO_3$ and $CoCO_3$: (a) $y = 0.1$, (b) $y = 0.3$ and (c) $y = 0.5$.

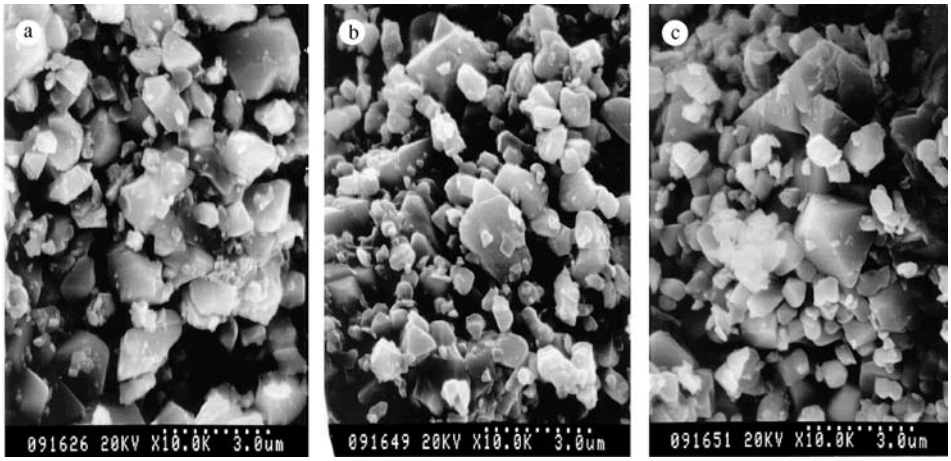

Fig. 8. SEM micrographs of $LiNi_{1-y}Co_yO_2$ synthesized at 800 °C using Li_2CO_3, NiO and Co_3O_4: (a) $y = 0.1$, (b) $y = 0.3$ and (c) $y = 0.5$.

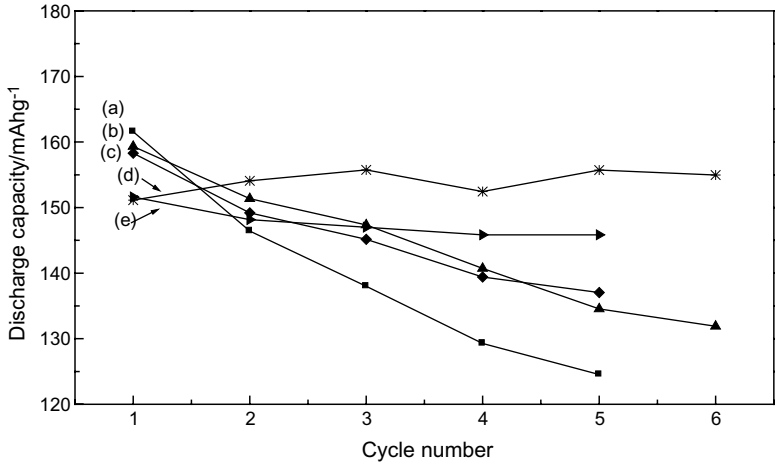

Fig. 9. Variations of the discharge capacities with the number of discharge cycle for samples having first discharge capacity larger than 150 mAh g^{-1}: (a) $LiNi_{0.7}Co_{0.3}O_2$ synthesized at 800 °C from $LiOH \cdot H_2O$, NiO and Co_3O_4, (b) $LiNi_{0.5}Co_{0.5}O_2$ synthesized at 850 °C, (c) $LiNi_{0.7}Co_{0.3}O_2$ synthesized at 800 °C (d) $LiNi_{0.9}Co_{0.1}O_2$ synthesized at 850 °C from Li_2CO_3, NiO and Co_3O_4 and (e) $LiNi_{0.9}Co_{0.1}O_2$ synthesized at 800 °C from $LiCO_3$, $NiCO_3$ and Co_3O_4.

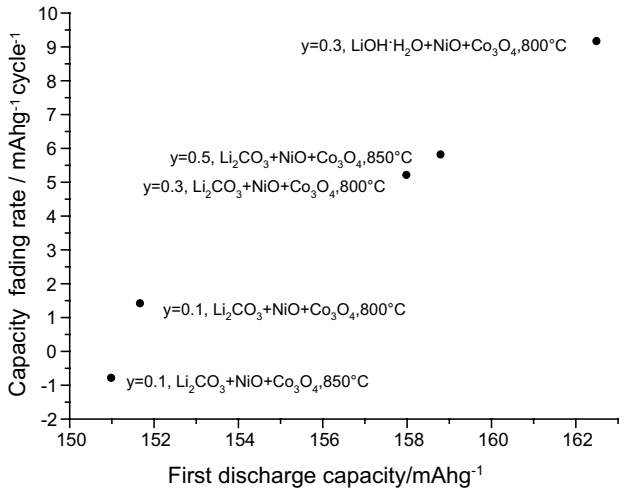

Fig. 10. Variation of capacity fading rate with the first discharge capacity for the samples having first discharge capacity larger than 150 mAh g^{-1}. Starting materials and the synthesis temperature are indicated.

larger capacity fading rate of the samples with the larger first discharge capacities.

4. Conclusions

$LiNi_{1-y}Co_yO_2$ samples were synthesized at 800 °C and 850 °C, by the solid-state reaction method, using various starting materials $LiOH \cdot H_2O$, Li_2CO_3, NiO, $NiCO_3$, Co_3O_4 and $CoCO_3$. The $LiNi_{1-y}Co_yO_2$ synthesized using Li_2CO_3, NiO and Co_3O_4 exhibited the α-$NaFeO_2$ structure of the rhombohedral system(space group $R\bar{3}m$). As the Co content increased, the lattice parameters *a* and *c* decreased. The reason is that the radius of the Co ion is smaller than that of the Ni ion. The increase in c/a shows that a two-dimensional structure develops as the Co content increases. $LiNi_{0.7}Co_{0.3}O_2$ synthesized at 800 °C using $LiOH \cdot H_2O$, NiO and Co_3O_4 exhibited a larger first discharge capacity 162 mAh g^{-1} than the other samples. The $LiNi_{0.9}Co_{0.1}O_2$ synthesized at 850 °C using Li_2CO_3, NiO and Co_3O_4 showed excellent cycling performance. The samples with the larger first discharge capacity will experience a more severe lattice destruction, due to the expansion and contraction of the lattice during intercalation and deintercalation, than the sample with the smaller first discharge capacity. As the first discharge capacity increases, the capacity fading rate thus increases.

Acknowledgement

This work was supported by the Research Center of Industrial Technology, Engineering Research Institute at Chonbuk National University.

References

1. T. Ohzuku and A. Ueda, *J. Electrochem.* **141** (1991) 2927.
2. J.R. Dahn and J.N. Reimer, *J. Electrochem.* **139** (1992) 209.
3. M. Yoshio, H. Tanaka, K. Tominaga and H. Noguchi, *J. Power Sources* **40** (1992) 347.
4. J.M. Tarascon, H. Tanaka, K. Tominaga and H. Noguchi, *J. Power Sources* **43** (1993) 689.
5. K. Brandt, *Solid State Ionics* **69** (1994) 173.
6. B. Scrosati, *J. Electrochem. Soc.* **139** (1992) 2776.
7. J.R. Dahn, U. von Sacken, M.R. Jukow and H. Aljanaby, *J. Electrochem.Soc.* **138** (1991) 2207.
8. K. Ozawa, *Solid State Ionics* **69** (1994) 212.
9. M.Y. Song and R. Lee, *J. Power Sources* **111**(1) (2002) 97.
10. M.M. Thackeray, W.I.F. David, P.G. Bruce and J.B. Goodenough, *Mater. Res. Bull.* **18** (1983) 461.
11. A. Momchilov, V. Manev and A. Nassalevska, *J. Power Sources* **41** (1993) 305.
12. G. Pistoia and G. Wang, *J. Electrochem. Soc.* **66** (1993) 135.
13. A. Yamada, K. Miura, K. Hinokuma and M. Tanaka, *J. Electrochem. Soc.* **142** (1995) 2149.
14. Y. Xia and M. Yoshia, *J. Electrochem. Soc.* **143** (1996) 825.
15. M.Y. Song and D.S. Ahn, *Solid State Ionics* **112** (1998) 21.
16. M.Y. Song, D.S. Ahn and H.R. Park, *J. Power Sources* **83** (1999) 57.
17. D.S. Ahn and M.Y. Song, *J. Electrochem. Soc.* **147** (2000) 874.
18. C. Delmas and I. Saadoune, *Solid State Ionics* **53–56** (1992) 370.
19. A. Ueda and T. Ohzuku, *J. Electrochem. Soc.* **141** (1994) 8.
20. M. Menetrier, A. Rougier and C. Delmas, *Solid State Communications* **90**(7) (1994) 439.
21. R. Alcantara, J. Morales and J.L. Tirado, *J. Electrochem. Soc.* **142** (1995) 12.
22. B. Banov, J. Bourilkov and M. Mladenov, *J. Power Sources* **54** (1995) 268.
23. A. Rougier, I. Saadoune, P. Gravereau, P. Willmann and C. Delmas, *Solid State Ionics* **90** (1996) 83.
24. Y.M. Choi, S.I. Pyun and S.I. Moon, *Solid State Ionics* **89** (1996) 43.
25. K. Kubo, S. Arai, S. Yamada and M. Kanda, *J. Power Sources* **81–82** (1999) 599.
26. E. Levi, M.D. Levi, G. Salitra, D. Aurbach, R. Oesten, U. Heider and L. Heider, *Solid State Ionics* **126** (1999) 97.
27. R.K.B. Gover, R. Kanno, B.J. Mitchell, A. Hirano and Y. Kawamoto, *J. Power Sources* **97–98** (2001) 316.